

NUMERICAL SIMULATION APPLIED TO THE AIR TEMPERATURE CONTROL AND IMPROVEMENT AT THE TLS

Jui-Chi Chang^{a,*}, Zong-Da Tsai^a, Ming-Tsun Ke^b

^aNational Synchrotron Radiation Research Center, Hsinchu, Taiwan

^bDepartment of Air-Conditioning and Refrigeration Engineering, National Taipei University of Technology, Taipei 106, Taiwan

Abstract

This paper presents the numerical simulation studies applied on the air temperature control and improvement at the Taiwan Light Source (TLS). To improve air temperature control and study the flow circulation in air conditioned areas, we had applied the computational fluid dynamic (CFD) scheme to the experimental hall, the storage ring tunnel, a technical zone and the booster area, respectively. We review those studies by examining the governing equations, the model construction, mesh generation, boundary conditions, convergence criterion and validation of simulations.

INTRODUCTION

It has been studied and verified that thermal effect is one of the most critical mechanical factors affecting the beam stability [1] [2]. The propagation routes from the temperature variation to the beam quality were also illustrated. Accordingly, TLS had made a series of thermal simulation and improvements on the air temperature control of the air-conditioning (AC) system for the storage ring.

The CFD technique has been applied for the heating, ventilating, and AC (HVAC) industry for more than 30 years since Nielsen [3] used the CFD technique to simulate flow motion in air-conditioned rooms. To more effectively and precisely predict the temperature variation and air flow in air-conditioned rooms, we had applied CFD technique to the experimental hall [4], the storage ring tunnel [5], a technical zone [6] and the booster area in TLS, respectively. All these four simulation cases are assumed as 3D, incompressible and turbulent flow.

We used FLUENT 6.2, a CFD code, to perform the numerical simulation. Both steady and transient states were simulated in all cases. Because most of HVAC industry flows are turbulent, we applied the k - ϵ turbulence model and SIMPLEC to solve the velocity and pressure problem. However, we are interested in the mean values rather than the details of turbulence.

GOVERNING EQUATION

The basic governing equations include the continuity equation, the momentum equation and the energy equation. They can be written in Cartesian-tensor form:

Continuity equation:

$$\rho_{,t} + (\rho U_i)_{,j} = 0 \quad (1)$$

Momentum equation:

$$(\rho U_i)_{,t} + (\rho U_j U_i)_{,j} = -P_{,i} - (\overline{\rho u_i u_j})_{,j} + \rho g_i \quad (2)$$

* E-Mail: jchang@nsrc.org.tw

Energy equation:

$$T_{,t} + (U_j T)_{,j} = (\alpha T_{,j})_{,j} + \Phi \quad (3)$$

where

t = time

ρ = density

U_i, U_j = mean velocity in x_i and x_j directions, respectively

P = pressure

$\overline{u_i u_j}$ = Reynolds stress

g_i = gravity acceleration in x_i direction

T = temperature

α = thermal diffusivity

Φ = dissipation function

MODEL CONSTRUCTION AND MESH GENERATION

FLUENT is composed of three parts, pre-processor, core operation and post-processor. GAMBIT, an integrated pre-processor, is used for geometry modelling and mesh generation. All the four simulated air-conditioned area are quite large with complex geometry. Appropriate simplification and modification of the actual geometries are needed to avoid skewed element in the process of mesh generation and to save computation time.

In the first simulation case, the experimental hall in the TLS is a donut-shaped area, of which inner and outer diameters and height are 29m, 80m and 11.7m, respectively. We divided this area into periodical symmetric six sections and only selected one of them to simulate. Yet there were 629,524 tetrahedron meshes were generated. The total volume of air (except solid equipment) is about $6.92 \times 10^3 \text{ m}^3$.

In the second case, the circumference of the TLS storage ring is 120m. The height of the storage tunnel is 2.8m. The geometries of some heat sources, such as magnets, insertion devices, vacuum and radio frequency chambers and the cable trays overhead were simplified. However, the simulated results would not be affected much due to those geometry simplifications.

In the third case, the circular-shaped technical zone is located on the core area of the storage ring. The diameter and height of the technical zone are 28.5m and 3m, respectively. All the heat sources of power racks, RF transmitters and low levels were modelled in the simulation. There are total 772,876 meshes generated in the air volume of $1.33 \times 10^3 \text{ m}^3$.

In the last case, there are a 50-MeV LINAC and a 1.5-GeV booster synchrotron located in the booster area. The circumference of the booster is 72m. All geometries of the magnets, RF system and cable trays were precisely

modelled. The mesh number of this case is greater than those of former three cases. There are total 1,351,304 meshes generated in the air volume of $2.76 \times 10^3 \text{ m}^3$. The mesh number and the total volume of air of these four cases are listed in Table 1.

Table 1: Mesh number and the total volume of air of four simulation cases.

Simulated Area	mesh number	total volume of air (10^3 m^3)
Experimental hall	629,524	6.92
Storage ring	316,050	1.06
Technical zone	772,876	1.33
Booster area	1,351,304	2.76

BOUNDARY CONDITIONS

Setting of boundary conditions is one of the most critical factors determining simulated results. Therefore, we set all boundary conditions as close to actual cases as possible. All the geometries, dimensions and locations of air exits and air exhausts were precisely modelled. In real cases, all the air exits in these four cases are opened on the ceiling. The air velocities at air exits were set according to actual site measured data, and the air exhausts were assumed as pressure outlet in all four cases.

Data of cooling load in most simulation cases were mainly collected from our utility archive system and estimated according to ASHRAE Handbook Fundamentals [7]. Some data of cooling load were surveyed from accelerator subsystems. For example, Table 2 shows power input and efficiency of equipment in the technical zone, which were provided by each subsystem.

Table 2: Power input and efficiency of equipment in the technical zone

Equipment	Power input	Efficiency
Transmitter I	120 kW	40 %
Transmitter II	120 kW	40 %
Low level	30 kW	90 %
SRF transmitter	200 kW	40 %
Dipole PS	450 kW	75 %
Quadrupole PS	7.5 kW x 18	80 %
Sextupole PS	19 kW x 2	75 %
Corrector PS	400 W x 18	30 %
Rack I, II	80 kW	90 %

CONVERGENCE CRITERION

Because of the truncation error of the numerical computation and differences of computed values resulted from the iteration, there exists small difference between two sides of the governing equation. This difference is known as the residual value. The residual value is used as the index of the convergence criterion in the numerical simulation. All the residual values of all physical parameters were set as 1×10^{-6} . If the residual value is not larger than 1×10^{-6} , the iteration was considered convergent.

SIMULATED RESULTS AND DISCUSSION

Figure 1 shows the simulated temperature contour for the experimental hall. Blue spots distributed on the ceiling show the air exits locations. Red zones distributed on the ceiling and the beam line indicate high temperature areas. The phenomenon of clear temperature difference demonstrates insufficient cooling capacity, which had been improved in the end of 2004.

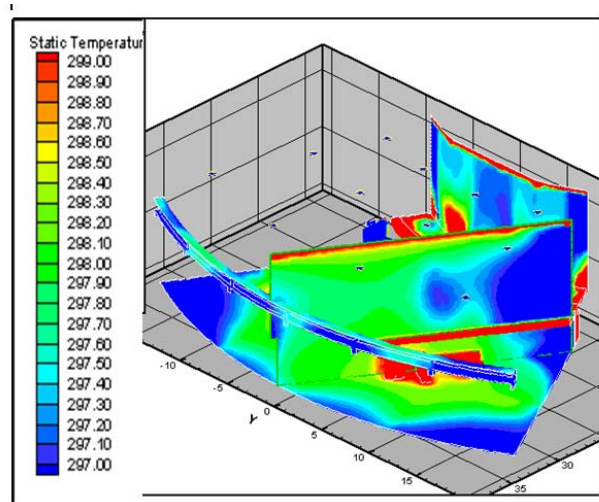


Figure 1: Simulated temperature contour for the experimental hall.

Figure 2 illustrates the simulated temperature contour and air velocity vectors on one cross section of the storage ring tunnel. It is shown that the high temperature areas are near the magnet and two cable trays overhead. Because all air exits and air exhausts are located on the ceiling, clear air flow appears on the upper zone in the figure. The global air temperature variation related to time in the storage ring tunnel is currently controlled within $\pm 0.1^\circ\text{C}$.

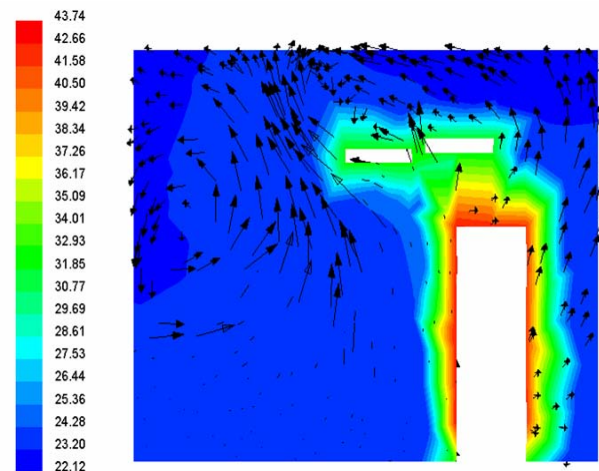


Figure 2: Simulated results of one cross section of the storage ring tunnel.

Figure 3 shows the simulated temperature contour for the technical zone. It is clear that the temperatures of three upper power panels, which all are RF transmitter, are higher than that of other equipment because those RF transmitters have large power input but low efficiency, as shown in Table 2. Some rectangular zones around the side wall are normally opened exits, which were also set as air exhausts. One virtual cross sectional plane in the figure shows lower temperature than that of equipment. We had compared some simulated temperatures with measured one on some specific locations. The average temperature difference between the simulated and measured results is about 1 °C.

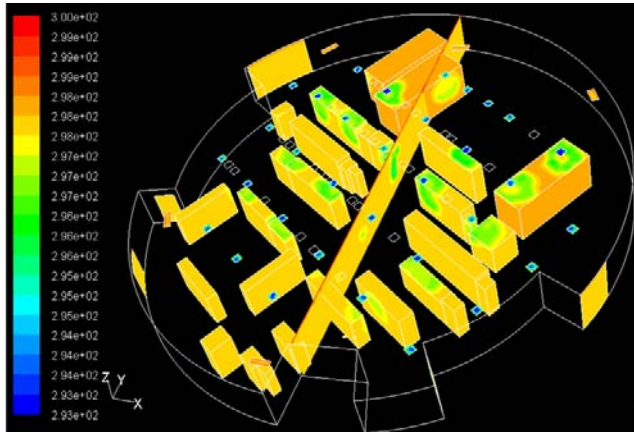


Figure 3: Simulated temperature contour for the technical zone.

Figure 4 and 5 respectively show the simulated temperature contour and air velocity vectors for the booster area. Temperature field along the whole booster is clearly demonstrated in Figure 4. The highest temperature area is located near the LINAC as shown the figure. The simulated global air temperature variation related to time in the booster area is about $\pm 0.15^{\circ}\text{C}$, which is close to the actual case. Figure 5 clearly illustrates the whole air flows, including flows from air exits on the ceiling and flows to air exhausts. A rectangular air exhaust on the left side is connected to the storage ring.

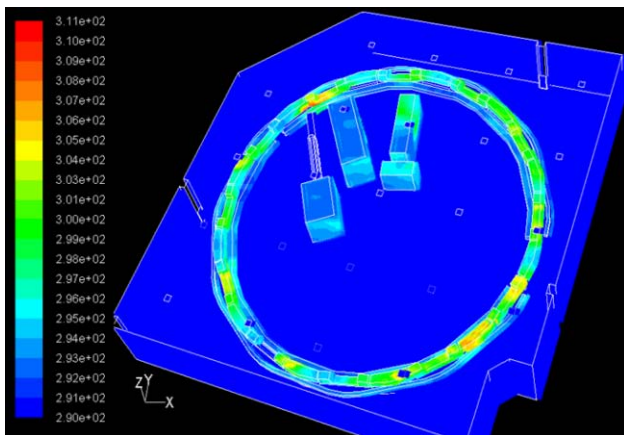


Figure 4: Simulated temperature contour for the booster area.

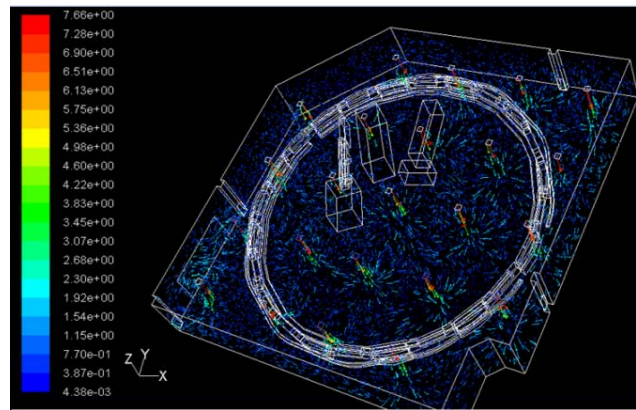


Figure 5: Simulated air velocity vectors for the booster area.

FUTURE WORK

We had simulated temperature field and air flow in the experimental hall, the storage ring tunnel, the technical zone and the booster area in TLS, respectively. Those simulated results had been validated by comparing with measured data. Those experiences will be further applied to designing the A/C system of our new accelerator, Taiwan Photon Source, TPS.

ACKNOWLEDGEMENT

Authors would like to thank colleagues in Utility, RF, PS and Vacuum groups of NSRRC for their assistance.

REFERENCE

- [1] J.R. Chen et al., "The Correlation between the Beam Orbit stability and the Utilities at SRRC", Proc. of 6th European Particle and Accelerator Conference EPAC98, Stockholm, Sweden, June 22-26, 1998.
- [2] J.R. Chen et al., "Mechanical Stability Studies at the Taiwan Light Source", 2nd Int'l Workshop on Mechanical Engineering Design of Synchrotron Radiation Equipment and Instrumentation (MEDSI02), APS, U.S.A., Sep 5-6, 2002.
- [3] Nielsen, P.V. 1974. "Flow in air-conditioned rooms." Ph.D. thesis, Technical University of Denmark, Copenhagen, 1974.
- [4] J.C. Chang et al., "Air Temperature Analysis and Control Improvement for the Large-Scale Experimental Hall" 2004 Asian Particle and Accelerator Conference (APAC), March 22-26, 2004, Gyeongju, Korea.
- [5] J.C. Chang et al., "Air Temperature Analysis and Control Improvement for the Storage Ring Tunnel" 2005 Particle and Accelerator Conference (PAC), May 16-20, 2005, Knoxville, USA.
- [6] J.C. Chang et al., "Air Temperature Analysis and Control Improvement for the Technical Zone at TLS" 2006 European Particle and Accelerator Conference (EPAC), June 26-30, 2006, Edinburgh, Scotland, pp. 1825-1827.
- [7] ASHRAE Handbook, Fundamentals, Chapter 28, 2001.